APPLICATION OF SHORT-TERM PRESSURE TRANSIENT TECHNIQUES FOR LOW-EMISSION TESTING

M.Y. Soliman, M. Azari and J. Ansah, Halliburton Energy Services, Inc.
C.S. Kabir, ChevronTexaco

ABSTRACT

In order to meet most test objectives, conventional transient well testing usually requires long flow and shut-in periods. However, the current industry drivers demand short, cost-effective, and environmentally friendly test procedures, especially in exploration wells. This is particularly true in deepwater and arctic environments where conventional tests may be prohibitively expensive or logistically not feasible.

While various short-term tests, test procedures, and interpretation methods are available for conducting successful short-term tests, clarity is lacking for specific applications of these methods. Some of these tests include surge testing, closed-chamber testing, slug testing, underbalanced perforating and testing, and back-surge perforation cleaning. This paper provides comprehensive evaluation of general closed-chamber tests, including general surge tests, and their comparison with special tests such as, FasTest,™ Impulse™ test, and slug tests. For each of these techniques, the review will examine:

- Test design, testing procedure
- Theoretical background of each of these techniques
- Method of data analysis including comparison based on both theoretical and practical considerations to determine the expected reliability, accuracy, and ease of analysis.

A large portion of the paper will be devoted to field examples. Several actual case studies are analyzed using the various techniques, and results are tabulated and presented. The analyses of several of these examples will be presented in significantly more detail to compare techniques available to analyze the well-testing data obtained from surge testing, closed-chamber DST, slug testing of oil wells, underbalanced perforating and testing, and back-surge perforation cleaning.

INTRODUCTION

Advances in gauge, tool assembly, and telemetry technology have collectively paved the way for the conduct of short-term tests. Some of these tests may last for time periods as short as a few minutes. Techniques developed for analysis of these tests rely on modem gauge capability for accuracy and quick measurement of pressure change with time as well as accurate compensation for the effect of temperature. These methods have been well established in the literature and include short-term tests such as:

- DST
- Slug test
- General closed-chamber test (CCT)
- Surge Test
- "Shoot-and-pull" test, which is similar to the backsurge test
- FasTest (essentially a surge test/CCT)
- Impulse Test (also essentially a surge test/CCT).

All the above tests with the exception of the slug test are similar in nature. Fluid flows into a limited volume chamber where an increasing back pressure causes the influx from the formation to decline. The decline in rate is very fast and is difficult and many times impossible to calculate. In many of these tests there is no differentiation between the flow and build up periods. This dictate the development of specialized techniques that turns accounts for this tests characteristic. In a slug test, however, flow is not against atmospheric pressure but against increasing hydrostatic head as fluid accumulation takes place. It is usually possible to calculate the rate production of fluid into the wellbore. This would allow for the use of classical analysis approaches if one wishes to.

The goal of this paper is to provide comprehensive evaluation of general closed-chamber tests, including general surge tests, and their comparison with special tests such as FasTest, Impulse and slug tests. The paper will analyze the practical considerations of the various tests and analytical techniques to determine the expected reliability, accuracy, and ease of analysis.

TEST TYPES

DST. The Drill Stem Test (DST) is a frequently run short-term test that was introduced to the industry in 1926. An arrangement of tools and valves is carried to the bottom of the well on the drill string to allow a zone of interest to be isolated and selectively flowed and closed in. DST's are performed on wildcat wells, offsets, and on infill wells. Upon successful completion of a DST and analysis of the collected data, an operator should have a basis for decisions concerning further expenditures; i.e., completion, etc., on the zone. Typical information that DST's may provide includes effective permeability, skin factor, initial pressure, and fluid type present in the formation. In summation, the DST provides a temporary completion of a well so that a transient pressure test may be performed and valuable information collected with minimal expenditures.

DST's may be run in open or cased holes. There are several variations of tool strings that can be used depending upon operator requirements. Conceptually, all DST's are similar, and the following five components[1] are necessary:

- A drill string, which carries the DST tools downhole and serves as a conduit for produced fluids
- A packer, which isolates the zone of interest and relieves the formation of the hydrostatic overbalance due to the drilling or completion fluid thus allowing formation flow
- A perforated pipe, which provides a path through which fluids may flow from the reservoir into the drill string
- A test valve, which provides the means to allow the reservoir to flow or to close in as needed
- A pressure gauge, which provides a pressure record of the test and a cross-check when difficulties are experienced.

DST flow-period bottomhole-pressure data are rarely able to be analyzed using conventional methods. For gas zones, the rate seldom stabilizes in the short time allotted for production. Therefore, gas well DST flow-period bottomhole pressures are not frequently analyzed; however, surface pressures are used in conjunction with surface equipment to determine gas rate for buildup analysis. Semi-log methods are preferred in the analysis of DST pressure buildup data as long as semi-log data exist.

Many liquid wells will not flow to the surface during the allotted production time on a typical openhole DST with an open surface valve. On such wells, the flow period becomes a slug period in which the increasing hydrostatic pressure exerted by the liquid causes the bottomhole pressure to increase as the pipe fills. On liquid wells that exhibit slug flow, the rate will be determined by the pressure data or the reported liquid recovery in feet or barrels if the recovery is reversed out to a tank. Gas wells often flow at the surface, and the rate may be based on surface conditions. Analysis of slug period will be discussed in next section.

Figures 1 to 3 present theoretical responses for various one-flow/one closed-in oil-producing DSTs. In **Figure 1**, the hydrostatic pressure buildup occurs more quickly during the slug flow period for the high permeability case. Skin damage will inhibit the productivity. The pressure increases slowly because of the slower rate of liquid influx into the pipe for the damaged case (**Figure 2**). However, the buildup occurs more rapidly for the damaged case. **Figure 3** shows the differences in behavior for a low permeability case with different skin factors.

DST usually has multiple flow and shut in periods. The first flow and shut-in period are usually short and serve to relieve super charge, but they also provide a basis for comparison. The second flow and shut-in period are analyzed for formation permeability and skin factor. Since the flow rate during the flow period could be changing quickly with time, it is advisable to consider this factor in the analysis. Rather than use average rate, one may use superposition[2] with time or the continuous change of rate with time.[3] The latter technique depends on the ability to getting a representative description of rate with time, and it provides better estimate permeability and skin factor.

Slug Test. Ferris and Knowles[4] first introduced slug testing in the field of groundwater hydrology in 1954. Allowing a reservoir to produce liquid into tubing or drill collars/drill pipe while open at the surface constitutes a slug test. As hydrocarbon flows into the drill pipe, the backpressure against the formation increases, causing the flow rate to decline. Thus, both rate and pressure are changing during this test. This is similar to what happens during the flow period of a DST; however, in this case, the flow period is an extended period. Once liquid flows at the surface, slug flow no longer exists, and true pressure drawdown commences. The only technical difference between slug and surge tests is that surge tests employ a closed surface valve or closed chamber. Both tests are backpressure tests, but due to the closed chamber and air compression, surge tests build back to static reservoir pressure faster than slug tests.

Slug tests are not frequently used, and probably occur by accident rather than by design. Theoretically, fluid samples, permeability, skin, and initial pressure should be available with a slug test; however, certain analyses techniques may preclude determination of initial pressure or skin.

Analysis of slug tests was introduced by Ramey *et al.*[5] In their analysis of the flow period of a DST test, fluid flows into a pipe. The rising liquid level in the drill pipe causes an increased back pressure against the formation, which in turn, reduces the flow rate. The type curve presented by Ramey et al may be plotted in one of three formats. **Figure 4** is one of these formats and it is the most general.
The y-axis of type curve in figure 4 is defined as following:

$$p_D = \frac{p_i - p_{wf}}{p_i - p_o}$$

For a slug test all terms in the above definition are known meaning that the y-axis is defined at all time. Thus matching with the type curve is achieved by moving the observed data horizontally till a match is achieved. The match is used to calculate permeability of the formation and the skin factor of associated with wellbore.

Closed-Chamber Drill-Stem Test (CCDST). Alexander[6] proposed this modified version of the DST in 1977. While similar to the conventional DST, the closed-chamber DST uses a closed surface valve during the flow periods. Rigorous use of surface pressure changes (dp/dt) and liquid influx data allow calculation of gas and liquid rates. Normal analysis of pressure buildup data taken during the closed-in periods may proceed with the known rates. According to Alexander, CCDST offers greater security and safety over a standard DST, and the rates can be used to estimate flow times necessary for fluid recovery in order to design surface equipment for future conventional testing.

CCDST appears particularly suited to testing of low- permeability gas wells. The test provides permeability, reservoir pressure, skin, and a fluid sample. A bottomhole pressure/time trace of a common CCDST may resemble that of a DST. The aims of a CCDST do not differ from those of the DST, and the same information can be gained from either procedure. The CCDST simply provides a rigorous basis for rate determination, particularly for gas wells, along with the previously stated advantages of safety and security.

An attractive feature of CCDST is that the test may be switched to conventional DST; i.e., the surface valve may be opened at any point during flow periods. A common procedure is to start a test as closed-chamber, and then, to switch to open-surface flow during the second or subsequent flow periods. The prior DST discussion concerning length of flow and shut-in applies to CCDST. However, often a short first-flow period of 10 to 15 minutes is used. Alexander presents a detailed pre-CCT design for maximum fluid influx and corresponding expected surface pressure rise.

Semilog and type-curve methods are applicable to CCDST pressure-buildup analysis. The surface-pressure response during the flow periods (surface valve closed) provides an excellent indication of the fluid influx at the sandface. Alexander provides a methodology to determine if the surface pressure response is consistent with 100% gas production, 100% gas-free water production, or situations in between such as gassy water or liquid hydrocarbons. The surface pressure behavior may be predicted through the equation of state for gas and knowledge of the chamber volume. Rates may be determined by using the change in surface pressure with time and liquid influx. Several authors presented charts and/or equations for determining rate during CCDST flow periods.[6-9]

Back-Surge Test. The surge test is a limiting form of the previously described closed-chamber flow period. Originally conducted in offshore Gulf Coast wells, back-surge perforation washing, and underbalanced perforating served to cleanup the well, enabling high-productivity well completion. Recent advances in analytical techniques allow the surge-pressure data to be analyzed.

Surge tests are typically shorter than DST's but allow for a rapid initial assessment of a zone with a relatively small amount of production. The tests can provide good estimates for permeability and even better estimates of initial pressure. A fluid sample may be retrieved also.

Back-surge is usually performed with underbalance tubing- conveyed perforation (TCP). Underbalance TCP is performed to minimize wellbore damage and usually results in clean perforations and negative skin factor. When the formation is allowed to flow into a small lower-pressure chamber, the test is termed back-surge. In most cases, it takes only minutes for pressure to stabilize.

Shoot-and-pull is analogous to a perforation underbalance treatment. Perforations are shot underbalanced, and fluid is allowed to flow while downhole pressure is monitored. At one point, either a downhole or a surface valve is closed, and the pressure is continually monitored during the buildup period. In a closed chamber test, the formation is allowed to flow while the well is closed at the surface. One may calculate fluid-flow rate from surface pressure and simultaneously monitored fluid level.

METHODS OF ANALYSIS

Some of the methods that may be used to analyze short-term tests are superposition or convolution, FasTest technique, and Impulse test technique. A brief description of each of these techniques is discussed next.

Superposition. Rates calculated during the flow period are used in the superposition equation to get a superposed rate/time value for each pressure point. The superposition equation accounts for all previous rate changes at and before a given point in time.[2] BHP is plotted versus the superposition rate-time function on a semi-log graph. This superposition rate-time function equation is given as

$$X_j = \sum_{k=1}^{k=j} \left[{(q_k - q_{k-1})}/{q_{last}} \right] \log\left(t_j - t_{k-1}\right) \qquad (1)$$

Similar to the Horner plot, the formation permeability is calculated from the slope of the straight line and is given by

$$k = 162.6\, q_{last}\, B\, \mu / m\, h \qquad (2)$$

Once permeability is determined, skin is calculated at each point with

$$S_j = \left[(p_i - p_{wj}) - (m/q_{last})x_j\right] / \left[(m/q_{last})q_j\right] \qquad (3)$$

Convolution Technique. Simmons[10] and Simmons and Grader[11] extended the convolution technique presented earlier by Meunier *et al*[12] to short-term tests. Simmons derived the following equations describing closed-chamber tests or back-surge tests:

$$p_i - p_{wf} = m\left[\sum t + S^* q(t)\right] \qquad (4)$$

$$\sum t = [(q_1 + q_2)/2]\log(t_j) + \sum_{i=2}^{j-1}[(q_{i+1} + q_{i-1})/2]\log(t_j - t_i) \qquad (5)$$

where

$$S^* = \log\left(k/\phi\mu c_t r_w^2\right) + 0.87\, S - 3.23 \qquad (6)$$

$$k = 162.6\, \mu / m\, h \qquad (7)$$

Assuming that S^* is constant, a plot of p_{wf} vs. $\sum t + S^* q(t)$ should yield a straight line with a slope of *m*, which is inversely proportional to formation permeability as given in Eq. 7.

Unfortunately, S^* is a function of both skin and formation permeability. Therefore, several approximations as well as an iterative procedure had to be developed to be able to calculate the formation properties. This made the technique very complicated. Another fairly significant limitation of this technique is the use of logarithmic approximation in Eq. 4. These tests may be too short in some instances for this approximation to be valid. One may use the Ei-function to avoid this issue.

It may be also noticed that both the superposition and convolution techniques assume the presence of homogenous, infinite, and radial system.

FasTest Technique. This technique was developed especially for analyzing buildup tests with very short producing periods. Instead of using the principle of superposition to derive the solution for a buildup test, Soliman[13] included the change in flow rate into the boundary condition and directly solved the drawdown-buildup problem, which made it possible to see features of the solution that could not have been observed otherwise. Soliman found that a plot of pressure change versus time yields a straight line whose slope is a function of flow regime while its intercept with the y-axis is a function of formation permeability. Specifically, he found that the following equations describe the long term behavior of various models.

Radial flow equation:

$$p_i\text{-}p_w = \frac{1694.4 V_{ch}\mu}{kh}\left(\frac{1}{t_p+\Delta t}\right) \tag{8}$$

Linear flow equation:

$$p_i\text{-}p_w = 31.05\ \frac{V_{ch}}{h}\left(\frac{\mu}{\varphi c_t k L_f^2}\right)^{0.5}\left(\frac{1}{t_p+\Delta t}\right)^{0.5} \tag{9}$$

Bilinear flow equation:

$$p_i\text{-}p_w = 264.6\frac{V_{ch}}{h}\ (\mu)^{0.75}\left(\frac{1}{\phi c_t\, k}\right)^{0.25}\frac{1}{\sqrt{k_f w_f}}\left(\frac{1}{t_p+\Delta t}\right)^{0.75} \tag{10}$$

Spherical flow equation:

$$p_i\text{-}p_w = 2.9434\times 10^4 V_{ch}(\phi c_t)^{0.5}\left(\frac{\mu}{k}\right)^{1.5}\left(\frac{1}{t_p+\Delta t}\right)^{1.5} \tag{11}$$

Equations 8 through 11 may be cast in a generalized form given by

$$p_i\text{-}p_w = c\left(t_p+\Delta t\right)^{\mathrm{n}} \tag{12}$$

A graph of logarithm of $(p_i - p_w)$ versus logarithm of total test time (t_p + □t) should yield a straight line whose slope is a function of flow model. The slopes are –1, – 0.5, – 0.75, and – 1.5, if the flow regime is radial, linear, bilinear, or spherical, respectively. The intercept of the straight line is a function of formation permeability.

Because only the total produced volume appears in the above equations, one does not need to know the flow rate to apply the FasTest analysis. Furthermore, the time term represents the total test duration; that is, from the start of flow through the buildup period. Therefore, one advantage of the FasTest analysis technique is that no flow period delineation is needed, which is hard to discern in short-term tests.

The FasTest technique does not make any assumptions regarding line-source well. The presence of the straight line discussed above will not only indicate the flow regime but will also indicate whether the test is analyzable. In other words, the technique is not only an analysis technique but it is also a diagnostic tool.

Equation 12 may be rearranged in a familiar form given by

$$\left(p_i\text{-}p_w\right)\left(t_p+\Delta t\right) = c\left(t_p+\Delta t\right)^{n+1} \qquad (13)$$

During radial flow, Eq. 13 becomes

$$\left(p_i\text{-}p_w\right)\left(t_p+\Delta t\right) = c \qquad (14)$$

In this case, a plot of the right-hand side of Eq. 14 versus time will eventually yield a horizontal line indicting the onset of analyzable data. For simplification and brevity, the rest of the paper addresses the radial-flow regime only.

One may construe that an accurate value of the initial-reservoir pressure is needed to apply this technique as shown in Eq. 12. However, the use of a derivative plot[14] identifies the flow regime and allows estimation of formation permeability, without prior knowledge of initial-reservoir pressure. The derivative formulation of Eq. 14 is given by

$$\log\left(t^2\,\frac{\partial\, p_w}{\partial\, t}\right) = \log\left[\frac{1694.4V_{ch}\mu}{kh}\right] \qquad (15)$$

Equation 15 suggests that a plot of the left-side of Eq. 15 versus logarithm of t will yield a horizontal straight line indicating the presence of radial flow. The intercept of the straight line is inversely proportional to formation permeability. Furthermore, once the flow regime and formation permeability are determined from the derivative plot, one may use Eq. 8 to establish the initial-reservoir pressure. This is simply achieved from the intercept of the p_w versus $(1/t)$ graph. The analysis technique will be demonstrated with field examples.

Impulse Test. Ayoub *et al.*[15] published an article on analysis of an Impulse test. The Impulse test technique was developed for an instantaneous withdrawal of reservoir fluid followed by a buildup period. The solution is given below by (Eq.1 in Ref. 15).

$$\Delta t\left(p_i - p_{ws}\right) = \frac{3388.8Q_I\,\mu}{k\,h}\,p'_D \qquad (16)$$

Where Q_I is the total volume equivalent to V_{ch} in FasTest. When the semilog approximation is valid, p'_D will be 0.5, indicating that at such time Eq. 16 will be identical to Eq. 8.

To compare and contrast the FasTest with Impulse test, let us rearrange Eq. 8 in the following comparable form

$$\left(t_p + \Delta t\right)\left(p_i - p_{ws}\right) = \frac{3388.8V_{ch}\,\mu}{k\,h}\,p'_D \qquad (17)$$

A comparison of Eq. 16 and 17 reveals that the producing is absent in the Impulse test formulation given by Eq. 16. In other words, the Impulse test is a particular case of a FasTest formulation when instantaneous fluid withdrawal occurs; meaning shut-in time is much larger than producing time. In practice, however, the preceding assumption along with delineation of drawdown and shut-in periods may present a few problems. We, therefore, recommend the use of FasTest analysis to minimize both theoretical and practical issues.

ESTIMATING TEST DURATION FOR CCT

Economics, logistics, and HSE requirements often demand short-term tests, particularly in operationally challenging environments, such as in the arctic and deepwater. Questions immediately surface about the validity and usefulness of these tests because of shallow radius of investigation owing to small fluid withdrawal or injection. Economics also dictate the knowledge of inaccuracy introduced when tests are terminated prematurely so that additional zones may be tested or to simply save the rig time. Obviously, CCTs are appealing because no fluids are produced to surface.

To probe the appropriateness of CCT, a series of carefully designed tests reflecting the sensitivity of eight variables were set up. The primary goal behind these tests was to establish the total time needed to conduct these short-term closed chamber tests in order to effectively determine reservoir properties. Our ultimate objective was to develop simple correlations so that one could rapidly assess the time needed to conduct a CCT.

For this exercise, we developed a closed-chamber-test design model, which takes into account different design variables spanning across a wide range of reservoir as well as tool parameters. These parameters specifically include reservoir permeability, porosity, thickness, fluid viscosity, specific gravity, and compressibility as well as formation damage, chamber parameters, and underbalanced surge between the well and reservoir.

Table 1 presents the range of these variables, reflecting low or p-10 (10% probability of occurrence) and the high or p-90 (90% probability of occurrence). The analysis procedure is based on the FasTest derivative presented by Eq. 15. **Figure 5** shows a typical plot of the pressure response from one of the tests. A traditional log-log plot of the pressure change and well test derivative is presented in **Figure 6**, which shows a diagnostic negative one slope at the intermediate time, after wellbore storage response, for this radial flow system.

A re-plot of the pressure derivative response, reflecting the pressure derivative group given by Eq. 15, is presented in **Figure 7**. Observe from this figure that the end of wellbore storage is evident by the diagnostic horizontal straight line. As indicated earlier, the intercept of this horizontal line on the vertical axis is inversely proportional to permeability. In this test, a perfectly horizontal line, which characterizes formation radial flow, is attained at approximately 0.9 hrs into the test.

In order to determine the total test duration necessary for the establishment of an unambiguous straight horizontal line, a value of half logarithmic cycle beyond this point was selected for terminating the test. Results of the experiments are presented in **Table 2**.

We used the Plackett-Burman[16] experimental design to explore the relative sensitivity of these eight independent variables. The dependent variable is the time taken to develop one-half log-cycle worth of pressure data for the log-log, semi-log, or derivative analyses. **Figure 8** presents the Pareto chart showing the ranking of variables. The vertical line indicates that no variable is statistically significant within the 95% confidence interval because they all reside to the left of that line. However, we observe that four top variables are viscosity, permeability, chamber volume, and pressure-drop at the sand face. Ranking of curvature in the middle implies that nonlinear terms may be unimportant.

The positive sign associated with any variable implies that the dependent variable (test duration) will increase with increases in the value of this variable. In contrast, the variables with negative signs imply just the opposite. For instance, increasing permeability and drawdown (□p) will reduce test duration, while increasing viscosity, chamber volume, or skin will increase testing time.

Following this finding, we sought to answer an important question: What percent error in permeability estimates is incurred if the test is terminated one-half log-cycle sooner than the start of the semi-log line? Results from the study are summarized in **Table 3**.

In these numerical experiments, the average error in permeability estimation was about 12% with a minimum error of 4.5% and a maximum error of 24%. The resulting Pareto chart is very similar to Fig. 8 and is skipped here for brevity. This outcome is not surprising in that we merely moved the test termination point to one-half cycle sooner.

To develop simple correlations for use in estimating duration of short-term tests, we set up a three-level full-factorial design experiments with just two top variables – viscosity and permeability. That is because both the chamber volume and drawdown are really subset of the viscosity and permeability. **Figure 9** presents the Pareto chart based on these experiments. The dominance of viscosity is readily apparent from Figure 9.

We used permeability range of 300/700/1,000 md, and viscosity range of 1/5/20 cp to develop these correlations. These values reflect p-10, p-50, and p-90 occurrences. We obtain good correlations with only the linear terms. Therefore, the time required to achieve positive-one-half-cycle data in hours is given by:

$$t_{p_{1/2}} = 0.97 + 1.963\mu_o - 1.31\times10^{-04}\,k - 1.74\times10^{-03}\,\mu_o k \qquad (18)$$

And negative-one-half-cycle data in hours is given by

$$t_{mp_{1/2}} = 0.097 + 0.1963\mu_o - 1.31\times10^{-05}\,k - 1.74\times10^{-04}\,\mu_o k \qquad (19)$$

These correlations provide a very useful tool for estimating time required for testing, within the limits of the input variables. It allows a design engineer to very quickly design the testing time. Using a rigorous engineering approach, one may fine tune this time estimate.

Using the right design approach, Eq. 18, the expected error in estimating the test duration is less than 2%. On the other hand as shown in Table 3, Eq. 19 incurs a maximum error of 24%, with an attendant benefit of ten-fold reduction in test duration.

FIELD EXAMPLES

In this section, we present field examples illustrating various analysis techniques applied to the same and/or different test types. In particular, we selected examples such that multiple analysis methods may be used and that the results of short-term tests can be verified by the subsequent long-term tests. The intrinsic idea is to gain confidence in the results derived from short-term tests.

Example 1: CCT and Long-Term Tests. A series of tests, CCT/shut-in (10 min/90 min), followed by two sets of flow and shut-in tests (18.2/30.3 hours; 8.0/12.5 hours) were conducted in the Hebron Ben Nevis D-94 well in February 1999, offshore Canada. Formation tester data showed that the initial pressure, when extrapolated to the gauge depth, yielded 2,660 psia.

Figure 10 displays the pressure trace during influx of fluid into the CCT chamber. The instantaneous rates are inferred from pressure data by noting that single-phase oil flow occurs. This very short-term test lends itself to convolution or superposition treatment assuming that the line-source approximation holds in this case. **Figure 11** presents the pressure/pressure-derivative signatures of the convolved data. Forward simulation attests to the goodness of the match.

Subsequently, we used the 90-minute shut-in period data using the FasTest analysis method, as shown in **Figure 12.** The results so obtained are quite comparable with those obtained from the flow period.

Interpretation of the long-term tests shows the possibility of this well being in the vicinity of an aquifer, in concert with geologic interpretation. **Figure 13** presents the diagnostic log-log graph showing the late-time derivative behavior reflecting the mobility change. By favoring the longer of the two tests (BU-1), we sought a match of the overall history, as shown in **Figure 14.** Overall, a good match is indicated although a mismatch is apparent during the first drawdown. We surmise uncertainty associated with surface rate measurement precipitated this issue.

We observe consistent agreement in the permeability value obtained from all the analyses. Also, we note an excellent agreement in the p_i value between the long-term tests and that measured by the formation tester. However, the short term tests yield values that are well within engineering accuracy of formation tester data. Note that skin values obtained from short-term tests are usually less reliable than their long-term counterpart. This lack of reliability stems primarily from the fact that the formation has not had time to cleanup. Practically speaking, skin is less of an issue during a DST when one seeks a reservoir's intrinsic flow potential with a temporary completion.

Example 2: Shoot-and-Pull Test. A Shoot-and-Pull test was planned in conjunction with the perforation of an offshore well. As discussed earlier, the reservoir fluids flow into the wellbore inside the tubular under a controlled underbalance condition. Four high-resolution gauges were used to record the changes in pressure. Two of the gauges were located at 12,322 ft TVD and the other two were at 5,804 ft TVD. A 38-ft pay interval was perforated with a high-density 14-SPF gun. Under a controlled underbalance condition the reservoir fluids surged into an enclosed tubular at surface. During this surge test, 481 ft or 8.543 bbl of fluid was recovered between the upper and the lower multi-service valves inside the drill pipe. The upper gauges are located above the liquid gas contact, while the lower gauges are significantly below it. **Table 4** provides the reservoir and wellbore data.

Figure 15 shows the pressure profile of the perforation event and the subsequent surge occurring between the hours of 21:20 to 21:51 for one of the lower gauges. The surge period for the four gauges is displayed in **Figure 16**.

The flow rate and the bottomhole pressure during a closed-chamber surge test change continuously, thereby rendering the conventional well-test analysis a very difficult proposition. **Figure 17** shows the log-log plot of the surge period for the lower recorder. Although a decent derivative plateau is attained over a log cycle, the late-time curvature is a manifestation of lack of superposition or rate variation that went unaccounted for.

However, this superposition issue is skirted when one uses the total time ($t_p + \Delta t$) derivative of Eq. 13 for this short-term test. **Figure 18** displays the derivative graph in question. Alternatively, one can use Eq. 15 to generate the derivative graph. As Figure 18 suggests, the anticipated horizontal line is well defined, notwithstanding the data scatter arising from gauge resolution. **Figure 19** presents the corresponding Cartesian graph and Eq. 8 yields the desired initial pressure.

Consistent results were obtained for all the four gauges. Given the proximity of the two sets of gauges, differences in the absolute values in p_i and s are expected to occur. **Table 5** summaries the results of the analyses. The difference between the extrapolated pressures of the lower and upper gauges is the hydrostatic pressure between the the two groups of gauges. Since the lower gauges are closer to the perforation and situated below the liquid-gas contact, the skin factor calculated using the data from these gauges are significantly more reliable than the ones calculated using the upper gauges.

Example 3: Multitest DST in a Horizontal Well. A multitest DST was planned for a well comprising two standard pressure drawdown and buildup tests followed by a surge test. This horizontal well was completed with 780 ft of perforated liner, which was not cemented in a formation tilted 60 degree from the horizontal plane.

Four pressure gauges were used to record both the pressure and temperature for the entire DST. Two of the gauges were located below and the other two above the tester valve. The two gauges that were located below the tester valve were used for the analysis and **Figure 20** shows the entire history recorded with one of those gauges along with the results of forward simulation. **Table 6** provides the reservoir and wellbore data, and **Table 7** provides the flow rate history.

The first flow was initiated with 800-psi underbalance by opening the tester valve. The reservoir did not have sufficient energy to lift the oil to surface. The well was shut in at the tester valve, and the first pressure buildup was recorded.

Figure 21 shows the log-log graph of the first pressure buildup. During the first 0.54 hour of drawdown, 6.7 barrels of fluid was produced out of the formation. This small amount of fluid is not enough to detect the boundaries during the test. The storage constant of 5.64E-4 STB/psi, is very low, since the wellbore is full of completion fluid with very small compressibility. The latter part of the data in Figure 21 is deviated upward because of short-producing-time effect, which could be mistaken for boundary effects. **Table 8** provides the analysis results.

Injection of nitrogen through a coiled-tubing unit at 5,000 ft MD helped the well to flow during the second flow period. During this flow period oil reached the surface at a fairly constant rate of 1,228 STB/D, amounting to a cumulative production of 302.2 bbls in 7.163 hrs. **Figure 22** shows the log-log plot of the second buildup data. The higher- than-normal value for the calculated k_z/k_r of 1.77 can be attributed to the formation angle of about 60 degrees from the horizontal plane. **Table 9** presents the analysis results for the second pressure buildup test.

The tester valve was opened yet again for the third flow period. The well flowed until it almost killed itself while the choke manifold was shut-in. A total of 42.7 bbls of oil was recovered in the tubulars. This final flow period was treated as a closed-chamber test, and an appropriate analysis technique was used.

Figures 23 and **24** show the pressure and the derivative FasTest analysis technique for the data collected during the surge period. A reservoir pressure of 1,602.4 psi and an average permeability value of 3.575 md were obtained by this analysis technique.

Since the production time for the first flow period is very short a conventional analysis technique may produce erroneous results. This is specially true for horizontal wells where longer production time is required to pass the first radial flow part and obtain a representative value for the radial permeability. Thus, the formation parameters obtained from the first test may not be regarded as accurate and reliable as the 2nd test. The formation permeability obtained by the FasTest represents the first radial flow part, which is $(k_v.k_r)^{0.5}$.

Example 4: Slug Test and CCT. This final example describes two tests, a slug test and a CCT (4.17 hours/7.98 hours) that were run in series in an onshore cased-hole well.[17] This well was located in a tight water-bearing sandstone formation. The full pressure history is plotted in **Figure 25**. The slug test was analyzed in the original paper, which reported a permeability value of 0.475 md. The CCT (or buildup) was also analyzed with rate-normalized pressure technique, yielding a permeability value of 0.5 md.

In this paper, we present analyses of the same data using the various short-term test techniques outlined earlier. Horner analysis of the data, using the full calculated rate profile, is shown in **Figure 26**. This analysis yields permeability estimate of 0.501 md and an estimated initial-reservoir pressure of 8,513 psia. Using an average rate of 238 STB/D, the conventional Horner analysis yielded a permeability estimate of 0.670 md and initial reservoir pressure of 8,499 psia.

The same data was analyzed using the Impulse test analysis technique. Log-log plot of the data, according to Reference 14, is shown in **Figure 27**. The late time part of the data shows that the radial flow was not completely established owing to a meager 2:1 shut-in to producing time ratio. Analysis of the data yielded a permeability estimate of 0.573 md, using an initial pressure estimate of 8,532 psia. This value represents an upper bound of the permeability estimate, and will obviously reduce with more late time data.

Finally, the entire data was analyzed by the FasTest method. **Figure 28** is the FasTest derivative plot of these data. As mentioned earlier, the plot is independent of initial reservoir pressure. Figure 28 shows that the data have not fully reached the analyzable data yet, however it also shows that the test is very close to reaching the analyzable region for radial flow. This is apparent from the figure showing the data approaching a negative one slope straight line. As discussed in the numerical experimention section, the analysis of the data using the FasTest technique should be still acceptable.

Figure 29 presents the Cartesian plot of the data, which is used in determining the initial-reservoir pressure. In this case, $p*$ is estimated at 8,650 psia. As discussed earlier, this higher value is explained by the fact that buildup part of the CCT did not last long enough for the establishment of pure radial flow. Consequently, only the last few data points were used to establish $p*$.

Using the initial pressure value determined from **Figure 30** was developed. The figure presents the FasTest cartesian plot of the observed data, which also demonstrates the fact that this CCT was not run long enough. Strictly speaking, this example does not lend itself for the classical CCT analysis treatment; nonetheless, we wanted to explore the limits of the CCT analysis techniques. Drawing a diagnostic straight line through the last few data points yields a permeability estimate of 0.442 md, representing the lowest bound of permeability. Observe from Figures 28 and 30 that, had the test been run long enough, stabilization of the straight line would have resulted in a lower value for the y-axis intercept and consequently a higher permeability estimate. The resulting permeability estimate would potentially be closer to the 0.475 md reported by the slug analysis method, which considered continuous rate and pressure variation throughout the test.

A summary of all the analysis results is provided in **Table 10**.

DISCUSSION

This paper attempted to address short-term tests in a collective manner. In this context, we point out that both slug and closed-chamber tests involve changing rate and pressure at the sandface. Because slug tests are rooted in the groundwater literature, they are only suitable for low-energy oil reservoirs when flow does not reach the surface. By definition, slug tests experience a significant wellbore-storage-distortion period owing to constant-storage situation. By contrast, storage duration in all forms of CCTs is short-lived because of increasing fluid compressibility, precipitated by the oncoming reservoir fluids in a predetermined chamber volume. As discussed earlier, CCT is a preferred test from HSE standpoint, particularly in harsh environments, such as arctic or deepwater.

We have shown that short-term data analysis can be done in different ways to obtain comparable solutions. When variable rates can be measured or computed with a single[4] or two-phase[7] flow wellbore model, rate-convolution or superposition analysis can be done for the flow period. Of course, this rate history can then be used for doing conventional Horner or superposition analysis for the shut-in period. However, when rates cannot be easily inferred, use of the generalized short-term test solution becomes appealing. That is because only the recovered volume is needed, not the instantaneous rate. In addition, the total test time ($t_p + \Delta t$) is required, thereby relieving the analyst from having to discern the onset of shut-in period.

CONCLUSIONS

1. Short-term testing provides a comparable estimate of reservoir parameters as conventional tests. The presented field examples verify this point. In contrast, estimation of skin with CCT may not be reliable.
2. Simple correlations are presented for estimating the CCT test duration.
3. Numerical experiments show that half-log cycle of data beyond the start of the diagnostic straight line will give very accurate estimate of reservoir parameters. An order-of-magnitude of time saving can be realized when up to 24% error in permeability estimation can be tolerated.

NOMENCLATURE

c_t = total formation compressibility, psi
C = wellbore storage constant, STB/psi
B_o = oil formation volume factor, RB/STB
h = net pay thickness, ft
k = permeability, md
m = slope, psi/cycle
p = pressure, psi
p_D = dimensionless pressure
p_i = initial reservoir pressure, psi
p_w = wellbore pressure, psi
q = oil rate, STB/D
q_{last} = last oil production rate, STB/D
s = skin damage, dimensionless
ΔP_S = Pressure drop from skin damage, psi
s' = dimensionless skin and storativity term
t = time, hrs
t_p = producing time, hrs
Δt = shut-in time, hrs
T = reservoir temperature, °R
V_{ch} = produced volume into the chamber, bbl
X_j = superposition rate/time function, hrs
Z = real-gas deviation factor, dimensionless
γ_o = oil gravity, °API
μ = viscosity, cp
ϕ = porosity, %

REFERENCES

1. Fulton, D.D.: "A Primer to DST (Drill Stem Test) Chart Interpretation," 32nd Annual Southwestern Petroleum Short Course (Lubbock, Texas, 85.04.23-25) PROC PP 15-33, 1985.
2. Earlougher, R.C., Jr.: *Advances in Well Test Analysis*, SPE Monograph, **5,** 1977
3. Soliman, M.Y.: "New Technique for Analysis of Variable Rate or Slug Test," paper SPE 10083 presented at the 1981 SPE Annual Technical Conference and Exhibition, San Antonio, TX, Oct. 5-7.
4. Ferris, J.G. and Knowles, D.B.: "The Slug Test for Estimating Transmissibility," *USGS Ground Water Note,* **26** (1954) 1.
5. Ramey, J.J., Jr., Agarwal, R.G., and Martin, I.: "Analysis of 'Slug Test' or DST Flow Period Data," *J. Cdn. Pet. Tech.* (July-Sept. 1975) 37.
6. Alexander, L.G.: "Theory and Practice of the Closed-Chamber Drillstem Test Method," *JPT* (Dec. 1977) 1539.
7. Petak, K.R., Finley, D.B., and Coble, L.E.: "Drill Stem Test And Closed-Chamber Drill Stem Test Simulation," SPE 23115 presented at the Offshore Europe Conference held in Aberdeen, September 3-6, 1991.

8. Mfonfu, G., and Grader, A.: "An Implicit Numerical Model for the Closed Chamber Tests," SPE 19832 presented at the 1989 SPE ATM, San Antonio, TX, Oct. 8-11.
9. Kabir, C.S., Badry, R.A., and Hasaan, A.R.: "Two-Phase Gas/Liquid Flow Rate Estimation During Closed Chamber Testing," *J. Cdn. Pet. Tech.* (March-April 1991) 102.
10. Simmons, J.F.: "Interpretation of Underbalanced Surge Pressure Data by Rate-Time Convolution," *JPT* (Jan. 1990) 74.
11. Simmons, J.F. and Grader, A.S.: "Application of Closed-Chamber Theory to Backsurge Completion Testing," *SPEPE* (Nov. 1988) 527; *Trans.,* AIME, **285.**
12. Meunier, D.F., Wittmann, M.J., and Stewart, G.: "Interpretation of Pressure Buildup Test Using In-Situ Measurement of Afterflow," *JPT* (January 1985) 143.
13. Soliman, M. Y.: "Analysis of Buildup Tests With Short Producing Time," *SPEFE*, (August 1986), 363.
14. Soliman, M. Y. and Petak, K.R.: "Method Analyzes Pressure for Short Flow Times," *Oil & Gas J*. (April 30, 1990) 49.
15. Ayoub, J.A., Bourdet, D., and Chauvel, Y.: "Impulse Testing," *SPEFE* (September 1988) 534.
16. Plackett, R.I. and Burman, J.P.: "The Design of Optimum Multifactorial Experiments," *Biometrika,* vol. XXXIII, University Press, Cambridge, England (1943) 305.
17. Kabir, C.S.: "Seeking Synergy Between Drawdown and Buildup Analyses," *SPEFE* (June 1997) 125.

ACKNOWLEDGMENT
The authors of this paper would like to express their thanks to Halliburton Energy Services, Inc. and ChevronTexaco for allowing this work to be published. ChevronTexaco's Toyin Badru did the analysis for the numerical experiments and Larry Chrusch provided data and insights into interpretation of Example 1. We also thank Nancy Woods and Carolyn Williams for their efforts in preparing the manuscript.

FasTest™ is a trademark of the Halliburton Corporation
Impulse™ test is a trademark of Schlumberger

Table 1
Independent Variables for Plackett-Burman CCT Design

Variable	p-10	p-50	p-90
k, md	1	100	1,000
μ, cp	0.2	1	100
V_{ch}, bbl	1	10	20
Δp, psi	200	1,000	2,000
S	0	5	50
h, ft	10	50	100
γ_o, °API	15	25	40
ϕC_t, 1/psi	2E-4	2E-5	2E-6

Table 2
Results of CCT Design Experiments: Test Duration Based on One-Half Log-Cycle of Radial Flow

Run #	Estimated Time, hrs	Calculated k, md	Actual k, md	Error %
1	62.0	983.7	1,000	1.6
2	0.00042	1,006.1	1,000	0.6
3	155,000	1.0	1	1.1
4	0.62	1,001.2	1,000	0.1
5	0.29	989.5	1,000	1.1
6	100.0	993.7	1,000	0.6
7	3,400	1.0	1	1.4
8	130,000	1.0	1	0.8
9	22.0	1.0	1	0.9
10	6.50	994.9	1,000	0.5
11	95.0	1.0	1	0.5
12	28.0	1.0	1	0.6
13	2.8	99.3	100	0.7

Table 3
Results of CCT Design Experiments: Test Duration Based on Negative Half Log-Cycle of Radial Flow

Run #	Estimated Time, hr	Calculated *k*, md	Actual *k*, md	Error %
1	6.2	838.5	1,000	16.2
2	0.000042	1,117.9	1,000	11.8
3	15,500	0.9	1	8.7
4	0.062	1,049.2	1,000	4.9
5	0.029	848.1	1,000	15.2
6	10	879.1	1,000	12.1
7	340	0.8	1	24.0
8	13,000	0.8	1	15.9
9	2.20	0.9	1	14.0
10	0.65	955.1	1,000	4.5
11	9.50	0.8	1	15.3
12	2.80	0.9	1	6.7
13	0.28	88.9	100	11.1

Table 4 Reservoir, Completion, and Fluid Data for Example 2	
H, ft	38 TVD, 45 MD
Mid-Perforations, ft	12,582 TVD
T, °F	133
Packer depth, ft	12,493 TVD, 13,237 MD
Completion Fluid	10.7 lb/gal NaCl
Water depth, ft	4,856
Casing: P110	9.652", 53.5 lb/ft
Tubing: S135 Drill Pipe	5", 19.5 lb/ft, to 12,494 ft TVD
Air Chamber	481 ft @ 0.01776 bbl/ft, 8.543 bbl
Upper Gauge location, ft	5,804 TVD
Lower Gauge location, ft	12,322 TVD
Wellbore radius, ft	0.4
ϕ, %	25

Table 5
FasTest Analysis Results for Example 2

k_o, md	**p_i, psi** (extrapolated pressure)	**s**	**Analysis Type**	**Gauge**
77.2	6,515.2	-1.84	Pressure	1st Lower
77.0	-------	-1.85	Derivative	1st Lower
77.3	6,517.4	-1.88	Pressure	2nd Lower
77.0	------	-1.89	Derivative	2nd Lower
77.5	2,897.7	0.00	Pressure	1st Upper
77.5	------	0.00	Derivative	1st Upper
77.6	2,899.4	0.00	Pressure	2nd Upper
77.5	------	0.00	Derivative	2nd Upper

Table 6 Reservoir, Completion, and Fluid Data for Example 3	
ϕ, %	18
Hole size, in.	8.5
r_w, ft	0.354
h, ft	680
Gauge location, ft	6,259 MD or 5,137 TVD
Horizontal perforated liner, ft	6,345 – 7,125 MD
h_w, ft	732
Z_w, ft	143
Oil gravity, ^{o}API	25
B_o, RB/STB	1.14873
μ_o, cp	3.12
c_t, 1/psi	2.4076E-4
R_{si}, scf/STB	680
T, ^{o}F	130

Table 7
Flow Rate History for Example 3

Duration, hr	**q_o, RB/D**	**Produced Volume, bbls**
37.58470	0	0
0.04628	1,240	2.3911
0.06980	675	1.9631
0.19290	178	1.4307
0.23130	95	0.9156
19.99800	0	0
4.67754	1	0.1949
1.26600	10	0.5275
5.89596	1,228	301.677
24.31240	0	0
0.531156	1,000	22.1315
0.180104	800	6.0045
0.184029	600	4.6017
0.184028	503	3.8569
0.184025	325	2.4920
0.184028	211	1.6179
0.184024	138	1.0581
0.184027	84	0.6441
0.120706	60	0.3018
3.063330	0	0

Table 8 Parameters Calculated from Pressure Buildup # 1 for Example 3	
C, STB/psi	5.64E-4
S	1.45
Δp_s, psi	17.96
p_i, psia at gauge depth	1,608.6 @ 5,137 TVD
$k_o h$, md–ft	3,880
k_o, md	5.71
k_z / k_r	0.844
p_{wf}, psia	1,546.28

Table 9 Parameters Calculated from Pressure Buildup # 2 for Example 3	
C, STB/psi	0.0139
S	1.9
Δp_s, psi	450.1
p_i, psia at gauge depth	1,613 @ 5,137 TVD
$k_o h$, md–ft	2,630
k_o, md	*3.86*
k_z / k_r	1.77
p_{wf}, psia	920.4

Table 10
Analysis Results for Example 4

Analysis Type	**k_o, md**	**p_i, psia**
Slug Test	0.475	----
CCT with Horner Analysis (Avg. Rate)	0.670	8,499
CCT with Horner Analysis (All Rates)	0.501	8,513
CCT using Impulse Test Analysis	------	----
CCT using FasTest Analysis	0.442	8556

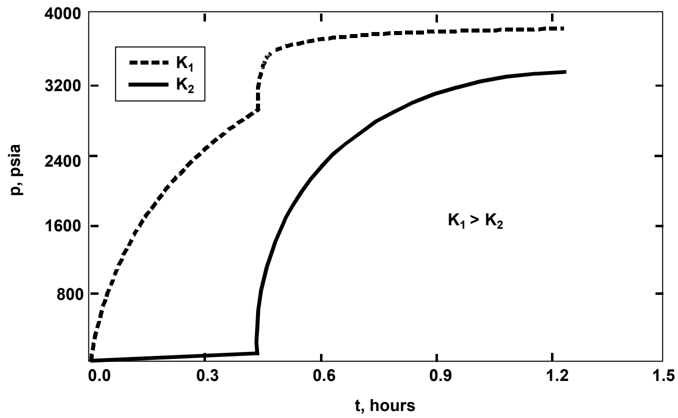

Figure 1 - Effect of Permeability on DST Behavior

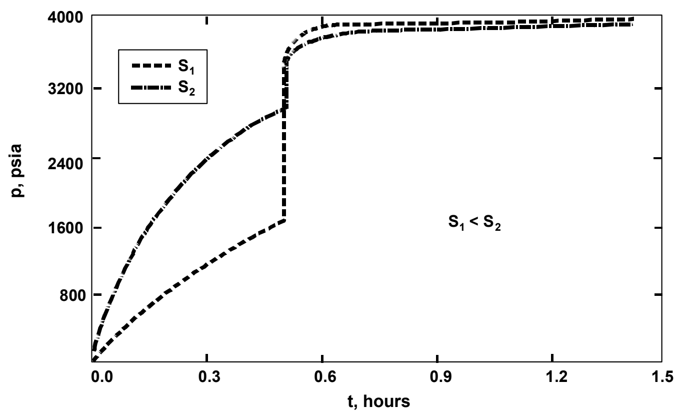

Figure 2 - Effect of Skin on High-Permeability DST Behavior

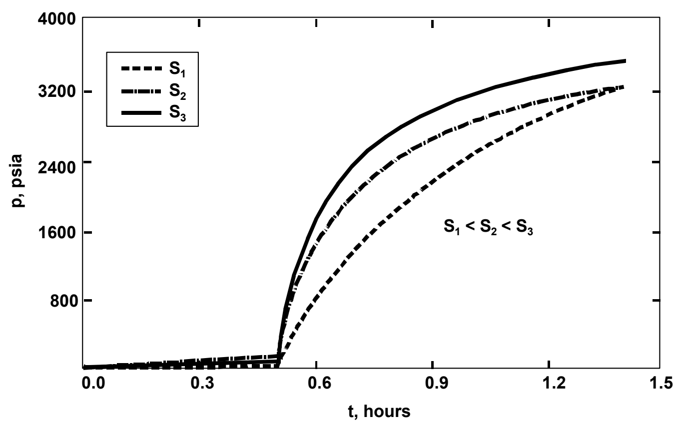

Figure 3 - Effect of Skin on Low-Permeability DST Behavior

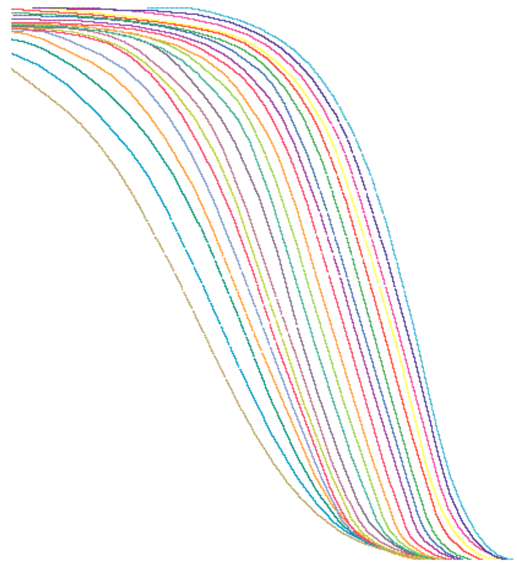

Figure 4 - Semi-log Type Curve for DST Flow-Period Data, After Ramey, et al.

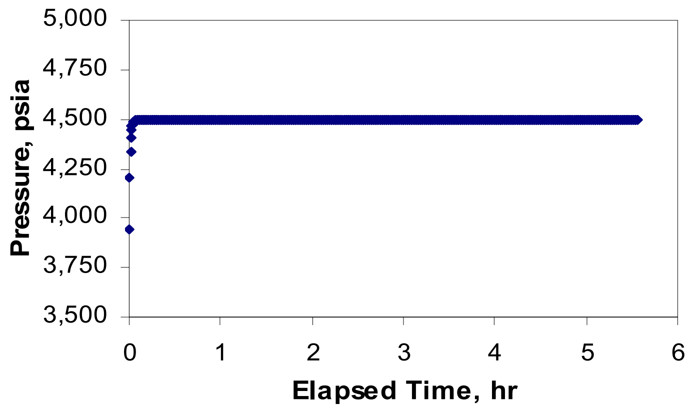

Figure 5 - Downhole Pressure Response of a Closed Chamber Test

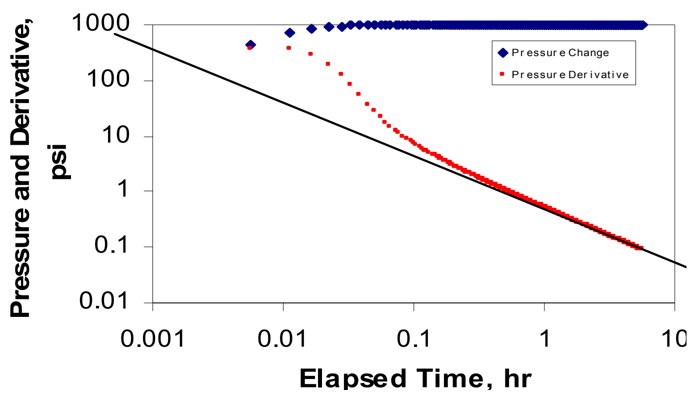

Figure 6 - Log-Log Plot of Pressure and Well Test Derivative Response of a Closed Chamber Test

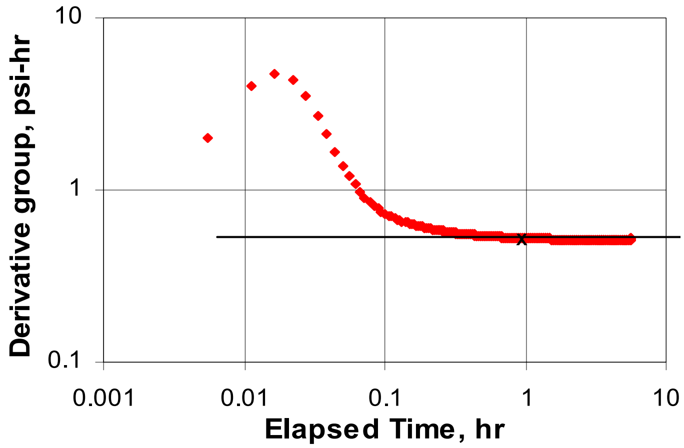

Figure 7 — Log-Log Re-Plot of the Derivative Response of a Closed Chamber Test (Eq. 15)

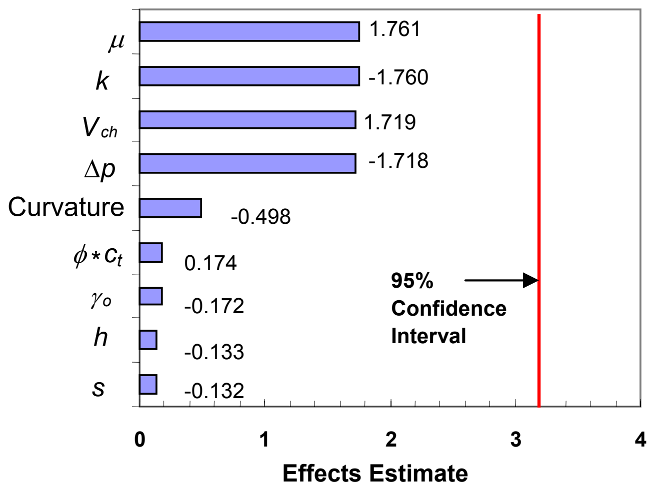

Figure 8 – Pareto Chart Shows Ranking of Variables In Half-Log-Cycle Evaluation

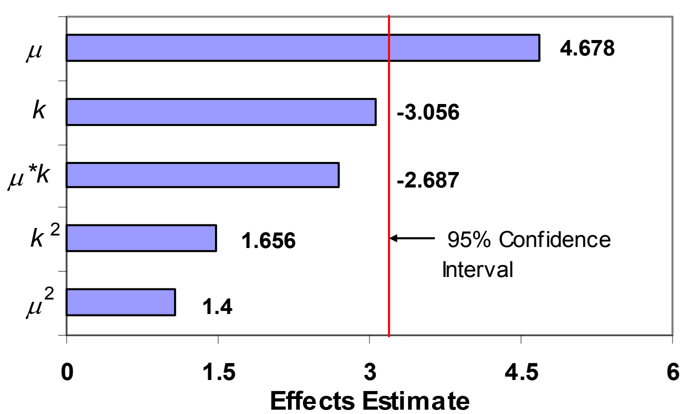

Figure 9 – Pareto Chart Shows Ranking of Variables In Half Log-Cycle Evaluation

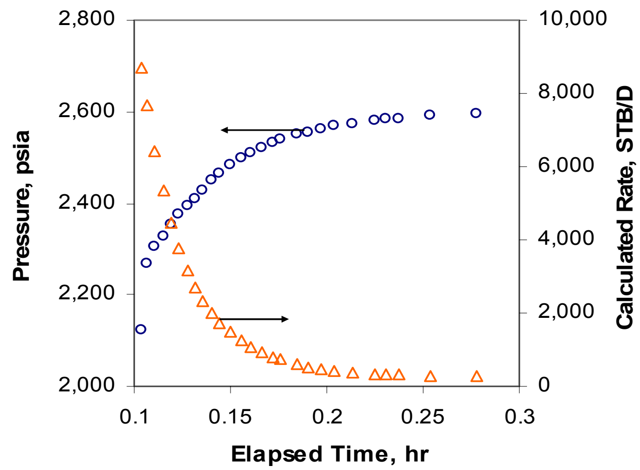

Figure 10 – Pressure and Computed Rate During the CCT Flow Period

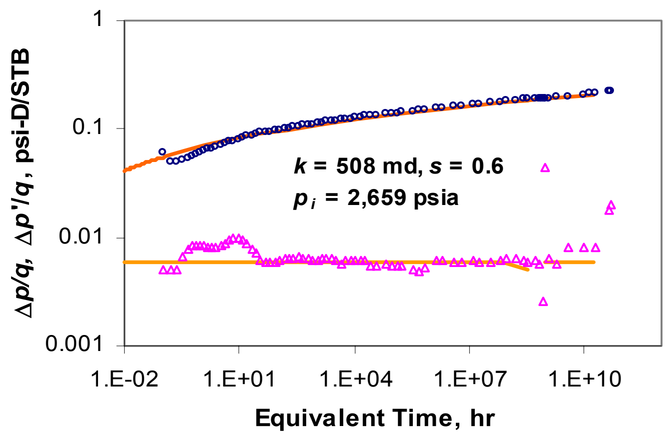

Figure 11 – Diagnosis and Analysis of CCT Flow Period Data

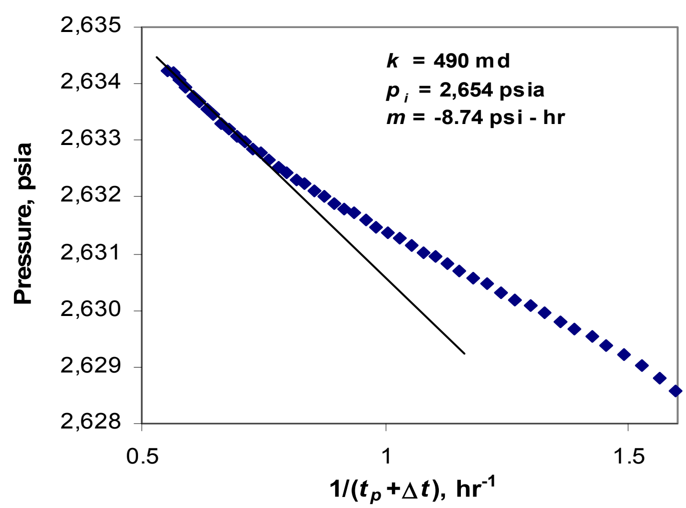

Figure 12 – Fastest Analysis of the CCT Shut-In Period Data

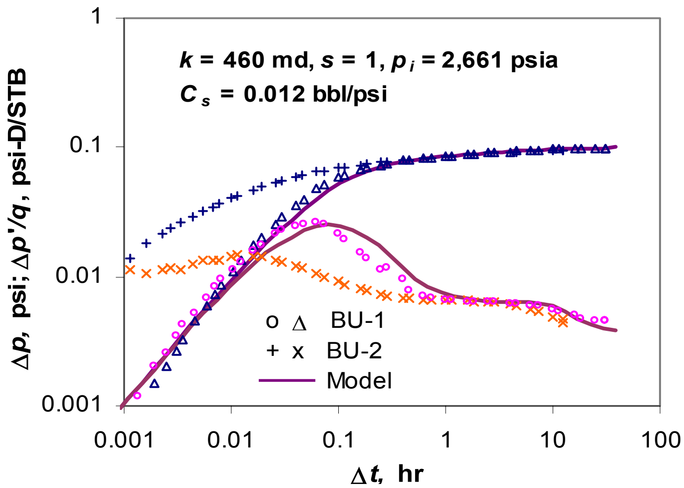

Figure 13 – Analysis of Two Long-Term Shut-In Tests

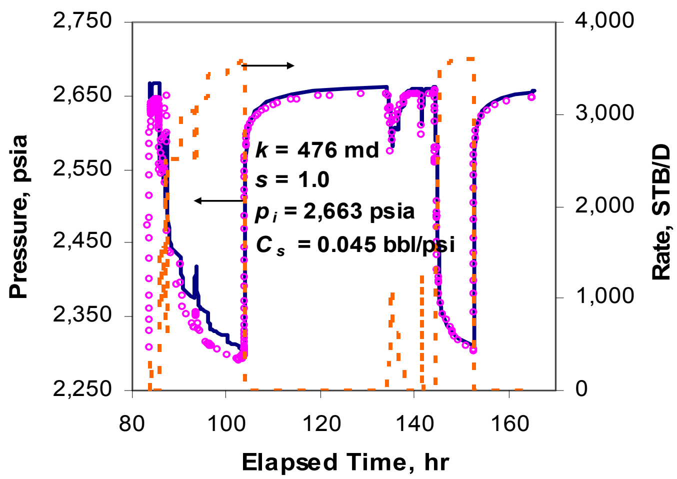

Figure 14 – History Matching of Overall Test Response

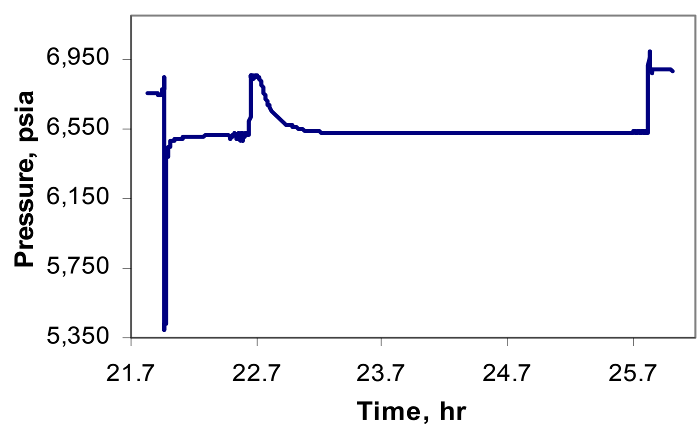

Figure 15 – Pressure Profile of the Perforation Event and the Subsequent Surge Response for Example 2 with the First Lower Gauge

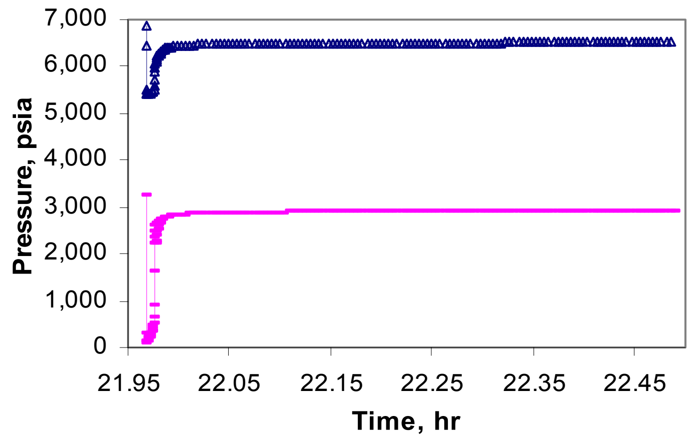

Figure 16 – The Pressure Profile of the Entire Surge Period for the Four Gauges of Example 2

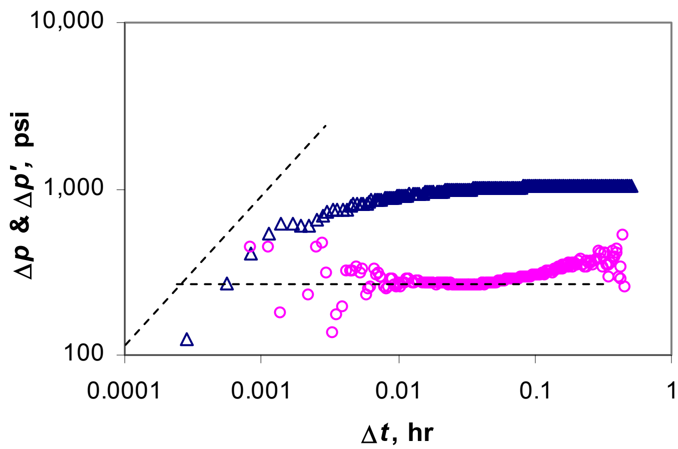

Figure 17 – Diagnosis of Surge Data for the First Lower Gauge of Example 2

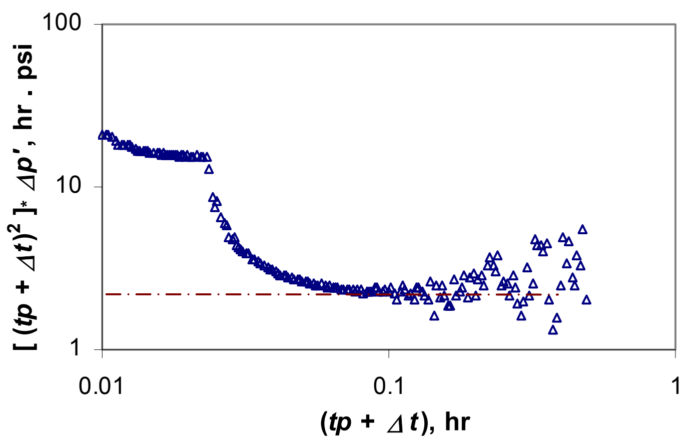

Figure 18 – The Fastest Derivative Plot of the Surge Data for the First Lower Gauge of Example 2

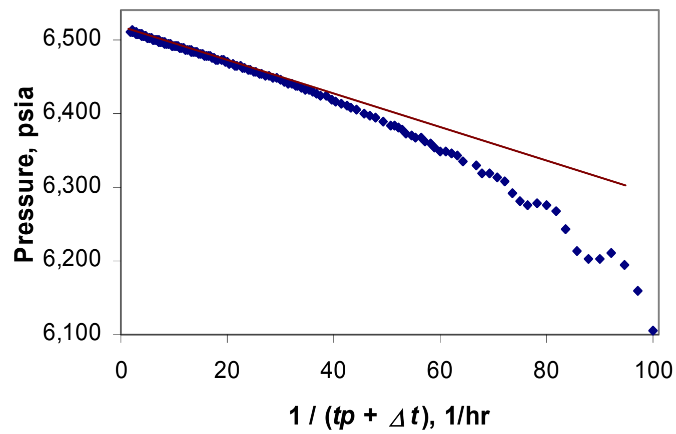

Figure 19 – Cartesian Graph for Estimating Pi From Surge Data for the First Lower Gauge of Example 2

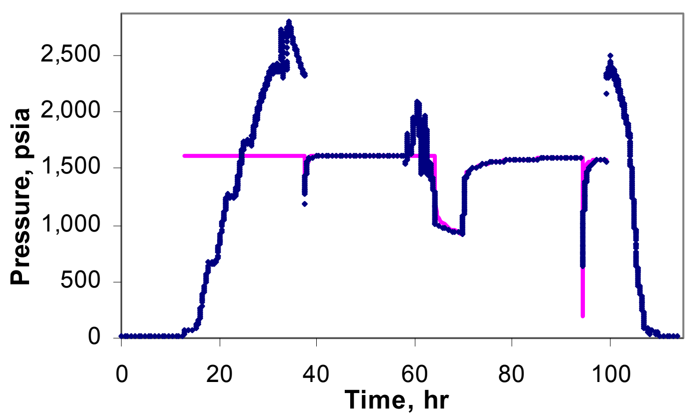

Figure 20 – Test History and Forward Simulation of Example 3

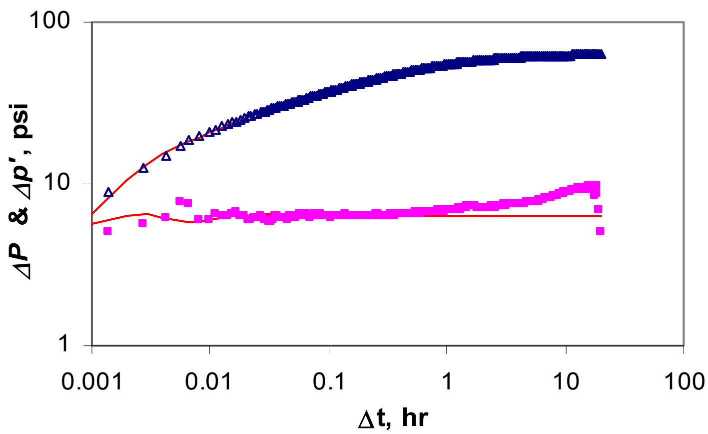

Figure 21 – Log-Log Diagnosis of the First Pressure Buildup Data of Example 3

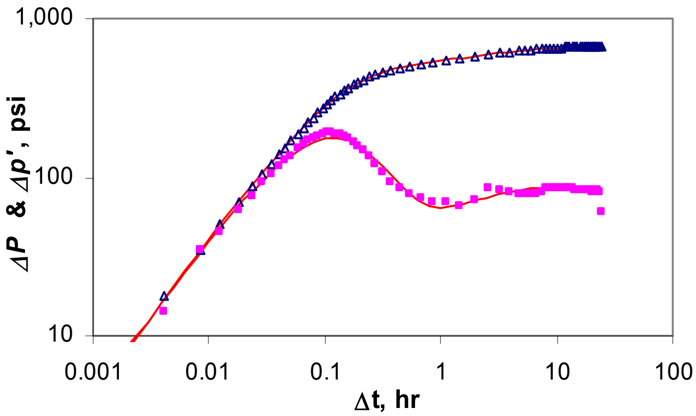

Figure 22 – Log-Log Diagnosis of the Second Pressure Buildup Data for Example 3

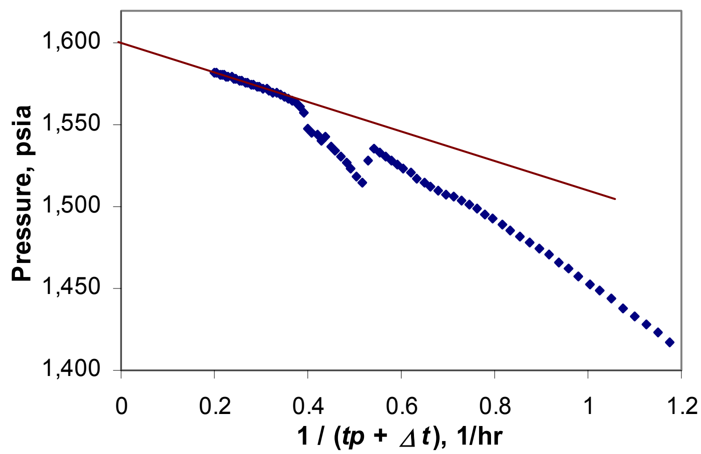

Figure 23 – The Fastest Plot of the Surge Data for Example 3

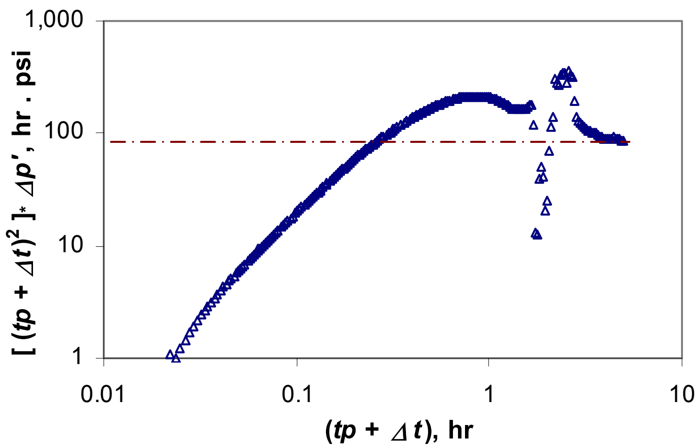

Figure 24 – The Fastest Derivative Plot of the Surge Data for Example 3

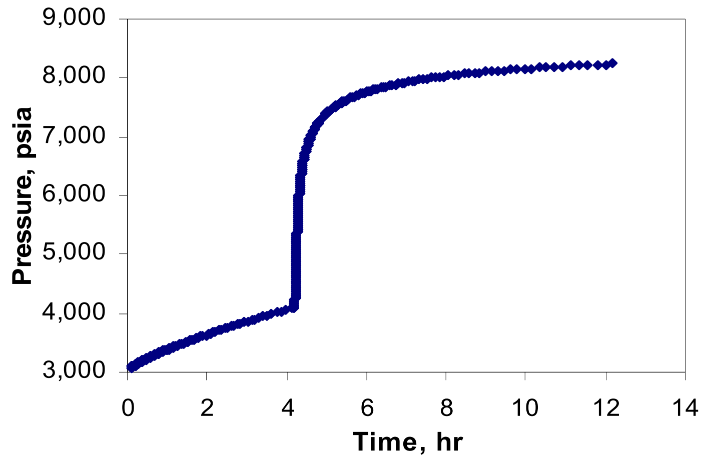

Figure 25 — Full Slug Test/CCT Pressure Profile for Example 4

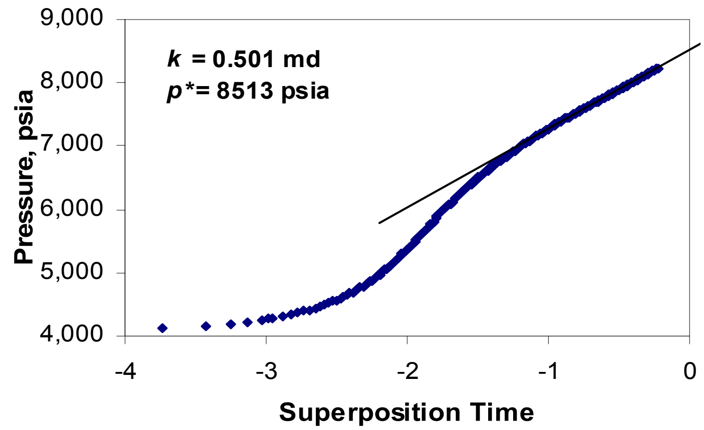

Figure 26 — Semilog Analysis of the CCT Data for Example 4

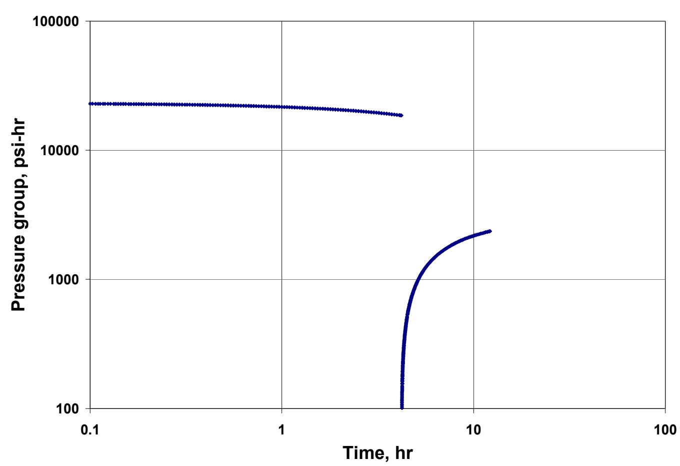

Figure 27 — Impulse Test Analysis of the CCT Data for Example 4

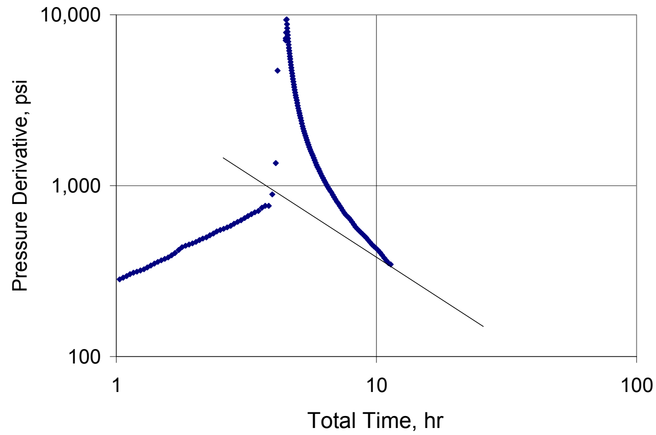

Figure 28 — FasTest Derivative Plot for the CCT Data for Example 4

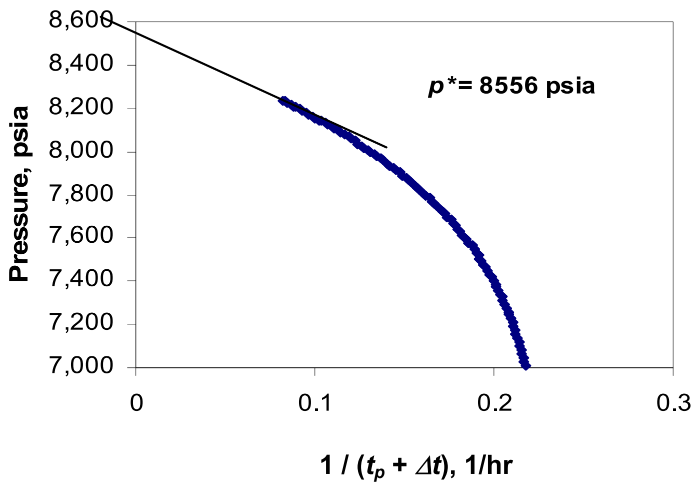

Figure 29 — FasTest Analysis of the CCT Data for Example 4

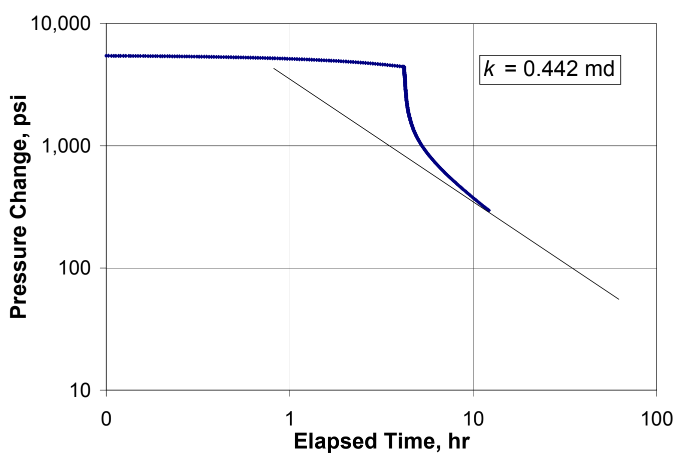

Figure 30 — FasTest Derivative Plot for the CCT Data for Example 4